Program Digest, 2019 IEEE International Ultrasonics Symposium (IUS)
Glasgow, Scotland, October 6-9, 2019

Arbitrary-Shape-Arrayed Aperture Fourier Beamforming in Arbitrary Coordinate System with No Approximate Interpolation

Chikayoshi Sumi
Dept of Info & Commun Sci
Sophia University
Tokyo Japan
c-sumi@sophia.ac.jp

Taku Asakawa
R & D division
Japan Probe Co., Ltd.
Kanagawa, Japan
taku.asakawa@jp-probe.com

***Abstract*—With the developed new approach, an arbitrary-shape-arrayed aperture Fourier beamforming can be performed in an arbitrary coordinate system without any approximate interpolations, for instance, direct generations of rf-echo data in a Cartesian coordinate system when using a convex or sector probe, or using a virtual point source set behind a linear-array-type probe, etc. In this report, the feasibility is confirmed for the 2D and 3D imaging through phantom experiments.**

Keywords—Fourier beamforming, arbitrary-shape-arrayed aperture, arbitrary coordinate system, no interpolation

I. Introduction

An ultrasonic Fourier beamforming is performed to achieve a higher speed processing than a precise phase-rotation delay-and-summation beamforming. To cope with sever artifacts generated by performing approximate interpolations of angular spectra by other groups, the author has been developing several approaches without the approximations; and the feasibility of the approaches have been verified through 3D or 2D imaging of wire or agar phantoms, etc [1]. One of our target was to make it possible to perform an arbitrary-shape-arrayed aperture Fourier beamforming in an arbitrary coordinate system without any approximate interpolations, for instance, direct generations of rf-echo data in a Cartesian coordinate system when using a convex or sector probe, or using a virtual point source set behind a linear-array-type probe, etc. [2]. This report confirms the method feasibility through phantom experiments.

II. Method

The approach performs the Jacobi operation for the Fourier transform of received echo data to yield the angular spectra directly in a Fourier domain corresponding to the target coordinate system. For instance, with respect to reception 2-dimensional (2D) echo signals rf(r,θ) expressed in a discrete polar coordinate system (r,θ), the angular spectra RF(X,Y) expressed for a discrete Cartesian coordinate system (x,y) can be calculated by implementing the Fourier transform with a Jacobi operation onto rf(r,θ) as follows:

$$RF(X,Y) = \iint_{x,y} rf(r,\theta)\exp(-j2\pi)(xX+yY)dxdy$$
$$= \iint_{r,\theta} rf(r,\theta)|r|\exp(-j2\pi)r(X\cos\theta+Y\sin\theta)drd\theta, \quad (1)$$

where |r| is Jacobian with respect to

$$x = r\cos\theta \text{ and } y = r\sin\theta. \quad (2)$$

Then, the Fourier-beamformed echo signals can be directly obtained in a discrete Cartesian coordinate system (x,y) by implementing the inverse fast Fourier transform (IFFT) onto RF(X,Y).

When using a point virtual source set behind a linear-array-type probe, delays are set for reception signals rf(x,y) in the Fourier domain by implementing phase rotations to yield rf(r,θ) virtually generated using a virtual circular-array-type probe. Such delays can also be implemented when performing the Fourier transform, i.e., eq. (1).

When using a spherical-array-type probe indeed or virtually, 3-dimensional (3D) echo signals rf(x,y,z) expressed in a discrete coordinate system (x,y,z) can be directly calculated with respect to reception 3D echo signals rf(r, θ,φ) similarly.

III. Phantom Experiments

For the 2D imaging, the new approach was verified experimentally for a cubic agar phantom with 100 mm sides. The phantom had in a 15 mm depth a 5-mm-diameter cylindrical inclusion having a higher concentration of an agar powder than the surrounding (7 and 3%). The graphite powder was added. Using a 1D linear-array-type probe (Ueda Japan Radio Co., Ltd., 7.5 MHz) was used with an rf-echo data acquisition system (Japan Probe Co., Ltd., 20 MHz). The probe was driven by 2 waves to acquire 256 × 4000 monostatic synthetic aperture (SA) data. An independent virtual point source was set behind the probe with different distances (r = 30, 60 mm) to virtually form 2 circularly 1D-arrayed aperture probes with different curvature radii r.

For the two curvature radii r, Fig. 1 shows images of an axial-lateral plane obtained by transmission and reception dynamic focusing. For both radii, the circular shape of inclusion was successfully imaged.

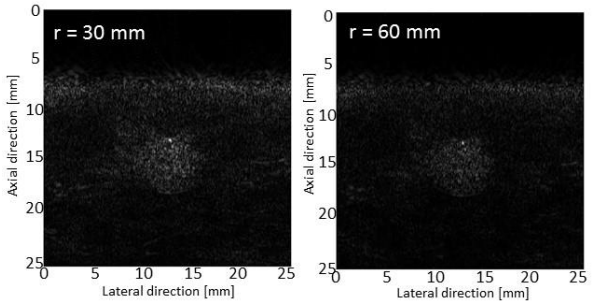

Fig. 1. For an agar phantom having an inclusion, echo images obtained using virtually, circularly 1D-arrayed aperture probes with 2 different curvature radii r = 30 and 60 mm via transmission and reception dynamic focusing.

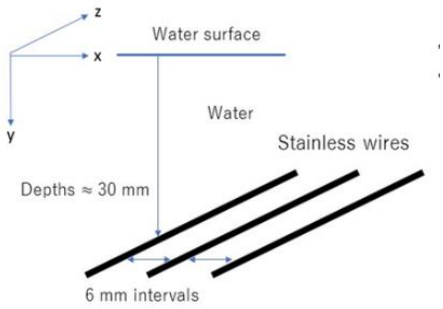

Fig. 2. Wire phantom.

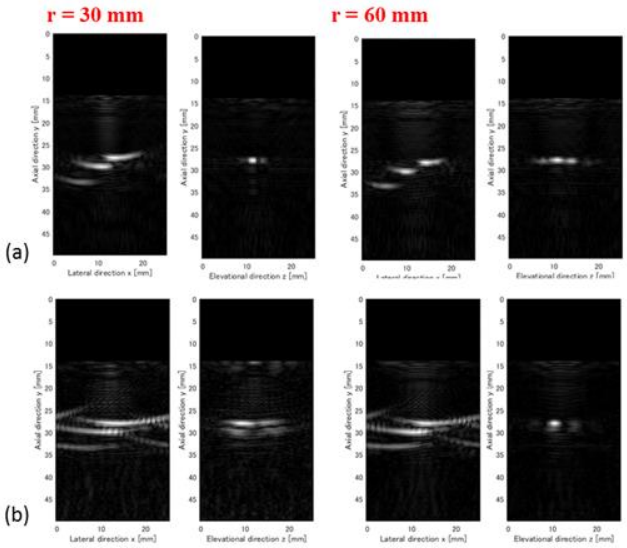

Fig. 3. Echo images obtained using virtually, spherically 2D-arrayed aperture probes with 2 different curvature radii r = 30 and 60 mm via (a) transmission and reception dynamic focusing; and (b) only reception dynamic focusing with respect to a spherical diverging transmission wave.

For the 3D imaging, the new approach was verified experimentally for wire phantom data used in [1,2]. Three stainless wires (0.23 mm-dia.) immersed about at a 30 mm depth (y) in a water with a 6 mm pitch in the x-direction and running in the z-direction (Fig. 2) were mechanically scanned by a 2D linear-array-type probe (Ueda Japan Radio Co., Ltd., 16 × 16 elements, 1.5 MHz, 0.4 × 0.4 mm pitches) set at the

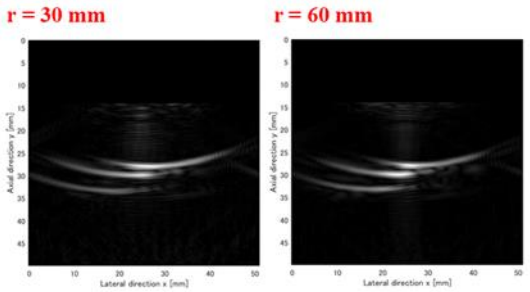

Fig. 4. Echo images with no lateral circulation artifacts shown in Fig. 3(b), which are obtained by padding zeros into the surrounding of raw echo data.

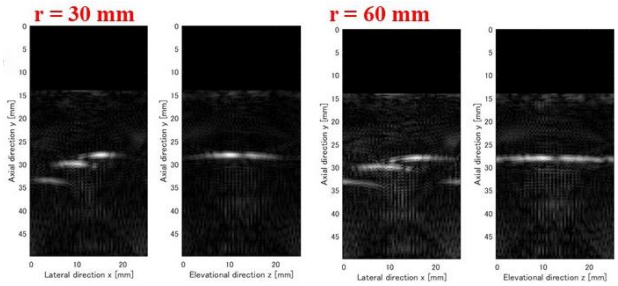

Fig. 5. Echo images obtained with delays artificially set during calculations for Fig. 3(a), i.e., eq. (1).

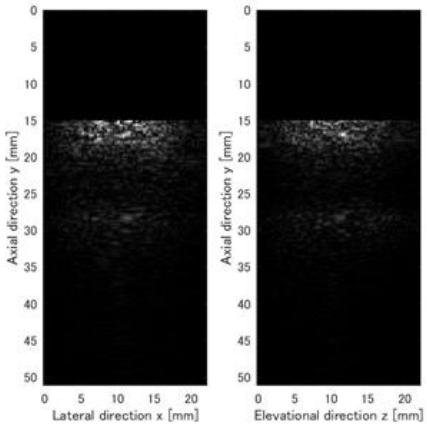

Fig. 6. For an agar phantom having a hole, echo images obtained using virtually, spherically 2D-arrayed aperture probe with curvature radius r = 60 mm via transmission and reception dynamic focusing.

surface of a water with the same rf-echo data acquisition system and a motorized positioner (Japan Probe Co., Ltd., 20 MHz) to acquire 64 × 64 × 1500 monostatic SA data. The probe was driven with 2 waves. Here, 2 independent virtual point sources were respectively set behind the mechanical scanning volume with different distances (r = 30, 60 mm) to virtually form 2 spherically 2D- arrayed aperture probes with different curvature radii r.

Figure 3 shows images of x-y and z-y planes obtained by (a) transmission and reception dynamic focusing; and (b) only reception dynamic focusing with respect to a spherical diverging wave transmission. In both beamformings, images of targets were successfully formed. Normally, r increasing, the lateral resolutions decreased; and the lateral resolutions were higher for (a) than (b). As shown in Fig. 4, the lateral circulation

artifacts shown in Fig. 3(b) were able to be coped with by padding zeros into the surrounding of raw echo data.

Next, delays were also artificially set during the calculations as mentioned above. For instance, with respect to Fig. 3(a), targets slightly pi-shaped in the x-y plane and running in the z-direction were clearly imaged as shown in Fig. 5. Such processing can also be categorized into a virtual source processing.

Finally, for the cubic agar phantom used in [2], a virtually, spherically 2D-arrayed aperture probe with a radius r = 60 mm was generated using the 2D linear-array type probe having 4 × 4 elements with an 8 MHz nominal frequency, 0.35 × 0.35 mm widths and 0.10 mm kerfs (Japan Probe Co. Ltd). The phantom (agar powder, 3%; graphite powder, 4%) with 100 mm sides having a cylindrical 10 mm diameter hole at a 20 mm depth was positioned at a 2 mm depth in a water. The hole ran in the elevational (z) direction. The probe was set at the surface of a water. 64 × 64 × 2048 monostatic SA data (a sampling frequency, 20MHz) were acquired by driving the probe with 4 waves. Figure 6 shows the result obtained with transmission and reception dynamic focusing.

IV. Conclusions

Using a virtual source set behind a 2D linear-array-type probe, image formations were experimentally achieved with respect to wire phantoms and agar phantoms. That is, rf-echo data were directly generated in a Cartesian coordinate system when using a virtual convex or sector probe without any approximate interpolations. This shows that an arbitrary-shape-arrayed aperture Fourier beamforming will be performed in an arbitrary coordinate system without any approximate interpolations.

In terms of a calculation speed, this Fourier beamforming is more effective in 3D than 2D beamforming (omitted). Similarly to our previously reported calculation for a plane wave transmission [1], by performing the calculation for the diverging wave transmission, single or plural physically arbitrary transmission waves can also be processed (not shown here). Next, various applications including for convex-type, sector-type, and deformable apertures will be reported. As shown in this report, point spread functions will also be controlled in a Fourier domain.

Acknowledgement

The traveling expenses are supported by The Precise Measurement Technology Promotion Foundation, Tokyo Japan.

References

[1] C. Sumi and T. Asakawa: Proc of 2018 IEEE Int Ultrason Symp (2018).

[2] C. Sumi: Jpn J Med Ultrasonics **46 Supplement** (2019) S557.